



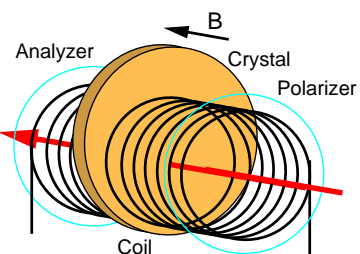
of 80 mW is spatially filtered and broadened to a diameter of about 30 mm.

We are imprinting the array configuration onto this beam with an amplitude modulator - a liquid-crystal diplay (LCD, 640x480 pixels) in amplitude mode driven by a computer graphics card. One example of a rectangular array configuration with 9x9 single beams is shown in the inset of figure 1. Moreover, the system allows to imprint arbitrary images on the beam, and we have therefore a very flexible tool for generating more or less complex spatial soliton configurations.

The spatially modulated beam is then demagnified and imaged onto the front face of the photorefractive Cerium-doped Strontium-Barium-Niobate crystal (SBN:Ce) we are using. To address the strong photorefractive nonlinearity the light is extraordinarily polarized in order to use the high photorefractive coefficient along the material's c-axis. A white light background illumination adjusts the dark conductivity of the material to prepare the conditions for soliton generation. With the help of an external electric bias field applied along the c-axis each of the array beams is able to produce a single solitonic waveguide. The distance of the single beams is chosen sufficiently large to avoid interaction between solitons.

Experiments on guiding beams of other wavelength in photorefractive solitons have been shown in [4, 7, 8]. In different soliton array configurations guiding of unmodulated beams with wavelengths 633 nm and 1.55  $\mu\text{m}$  has already been studied. Using this as starting point we have extended our setup to modulate the guided light beams to simulate data transmission in such a system.

The amplitude modulator we are using is based on a magneto-optic crystal (Yttrium-iron-garnet (YIG) film with Bismut[15]) which responds with Faraday rotation depending on an external magnetic field. Typical modulation frequencies of this material span up to Gigahertz range.



Modulation of the external magnetic field is performed using a long copper coil with about 20 turns that induces a relatively homogeneous field on its inside. The crystal is positioned in the center of the coil to ensure that the magnetic field is perpendicular to the crystal's surface[16]. The

FIG. 2: Schematic of the magneto-optical amplitude modulator setup. The red arrow indicates the beam propagation direction.

coil is placed between polarizing and analyzing polarizers to translate the polarization rotation into amplitude modulation of a passing light beam (see figure 2). As driver for the coil we use a music-amplifier with a maximum output power of 2 W that is connected

to a sound card output to permit for transmission of computer generated signals[17]. A red laser beam derived from a HeNe-Laser at  $\lambda = 632 \text{ nm}$  with 25 mW output power is amplitude modulated as described and focussed onto one of the beam positions on the front face of the photorefractive crystal to achieve coupling into the corresponding solitary waveguide.

The guided and therefore transmitted signal is detected using a photodiode that receives 90% of the light due to the semitransparent mirror in front of the camera where the other 10% are used for the imaging. We measure only the AC part of the current, the DC part is filtered with an electrical transducer behind the electrically amplified photodiode. A second amplifier matches impedance and amplitude of the electrical signal to the input of the computer's analog-to-digital-converter.

### III. EXPERIMENTAL RESULTS

#### A. General characterization

The first step to successfully transmit data with our setup is to generate photorefractive solitons in a suitable configuration for these experiments. A rectangular array of 7x7 solitons is chosen for easy addressing of neighbouring channels simply by moving the signal beam in horizontal or vertical direction. The array configuration is depicted in figure 3 (a). Because of the typical distance of the solitons of 80  $\mu\text{m}$  strong interaction between them is avoided, so that every beam generates an independent waveguiding channel created with an average light power of about 110 nW. The limiting factor of cross-coupling between parallel waveguiding channels does not depend on the temporal dynamics of the signal but on neighbouring waveguide distance. Therefore, in this article we investigate parallel beams with sufficiently large distance to avoid cross-coupling between channels in accordance to [7, 13]. The typical diameter of a single soliton is about 25  $\mu\text{m}$ . Nonlinearity is adjusted by an external electric field of 1 kV/cm applied along the c-axis of the crystal. Background illumination, beam power and external electric field are adjusted in order to allow for stable photorefractive soliton generation.

In agreement with earlier experiments, when large arrays of solitons are produced, the Gaussian shape of the beam illuminating the LCD and inhomogeneities of both the modulator and the crystal have to be considered. While the last two have a negligible influence in our case, the Gaussian light intensity distribution leads to larger time constants to reach stationary state for the solitons at the borders of the array compared with central ones. But due to saturation effect the same refractive index modulation is induced and therefore the same waveguiding properties are resulting. In order to confirm this, we first tested beam and signal transmission in different waveguiding channels successively and observed similar behaviour.

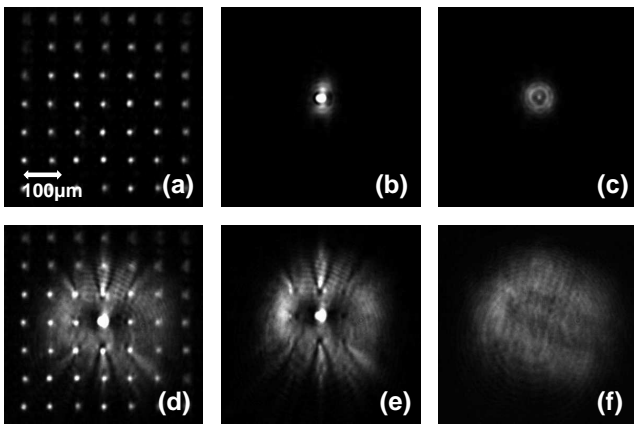


FIG. 3: Spatial filtering at crystals output face with a Gaussian beam guided in a  $7 \times 7$  array. (a) Array and beam together at output face of the crystal. (d) Array and beam together at output face of the crystal. Guided beam with (b) and without (e) spatial filtering with pinhole. Diffracting beam after waveguide removal with (c) and without (f) spatial filtering with pinhole.

To make sure we only receive and analyze the light that is being guided in the chosen photorefractive soliton we use an iris diaphragm ( $\simeq 30 \mu\text{m}$  diameter) placed directly at the output face of the crystal. This simulates a small aperture comparable to a large fiber input or a taper used for further transmission of the beam. In figure 3 we have displayed pictures of the output face with (b-c) and without (d-f) this spatial filter.

The time-resolved experiments themselves have been conducted using different pieces of music as input signal for amplitude modulation. The characteristics of this are typical for today's digital music systems. We have a frequency range from 20 Hz to 22 kHz (for the one stereo channel that we use) together with a dynamic range of 16 bit per sample. This gives a theoretical pulse length (when considering digital data transmission) of about  $45 \mu\text{s}$  and a data rate of 22 kbit/s. With our setup we cannot use the whole dynamic range of the original signal but can easily discriminate and analyze the different features of the system.

## B. Signal transmission analysis

To investigate the transmitted signal through one of the waveguides in the array we start recording the modulated light detected by the photodiode when the signal transmission begins. It is digitized by means of the analog-digital-converter in our computer. Figure 4 (a) shows the amplitude plot of the original piece of music as reference. In comparison the transmitted and recorded signal that undergoes several tests to determine the signal-to-noise-ratio and some other properties is depicted in figure 4 (b).

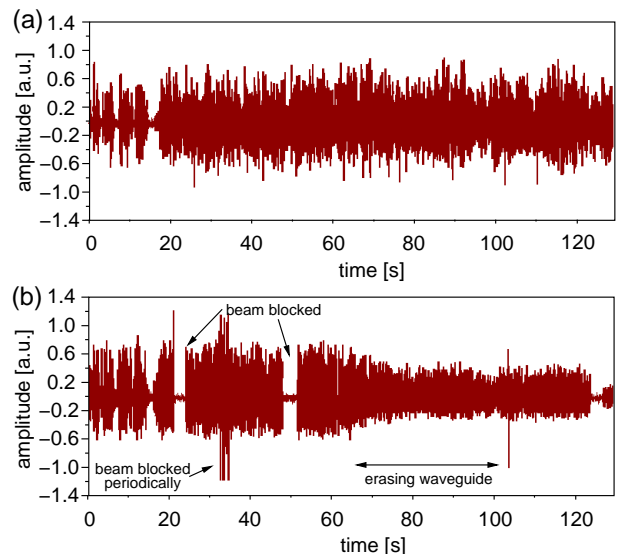


FIG. 4: Transmission of dynamic amplitude modulated signal. (a) shows the original piece of music for comparison, (b) the transmitted and then recorded version for analysis: The beam is blocked at 26 s to determine the signal-to-noise ratio. The dynamic range is studied at 37 s with periodic blocking of the beam. Erasing of the waveguide starts at 61 s and results in a reduced recorded amplitude (by about 50%).

In order to test the quality of the transmission in the spatial soliton, we performed several tests during transmission. The signal quality is determined by two main factors: the modulation depth that needs to be maintained as present in the original signal and the transmission of all frequencies present in the signal. Figure 4 shows some of the basic investigations related to that question. Properties like noise and modulation transfer of the system are considered.

At the beginning the strong even visible amplitude modulation during the first part (0 s to 20 s) is directly related to the artistic work. The noise level present in the system without signal transmission is primarily determined by the quality of the transmission setup which incorporates some internal and external noise sources. The photorefractive crystal and the solitary waveguides themselves are not creating any measurable additional noise. External light sources and power supplies operating in the same frequency range show a much stronger influence on the signal quality. The basic noise level without data transmission is depicted in figure 4(b) for example at the end starting from 124 s to 127 s.

From 22 s to 25 s the beam was simply blocked and unblocked again. This has been done to be able to differentiate between noise originating from the complete system including modulator and red laser in the first case from the detection unit in the second case. We found the difference to be negligible. The signal-to-noise ratio of this system is calculated to be 12 dB which is completely sufficient to study the fundamental features of the investigated system.

A second test here shows several spikes in the amplitude due to repeatedly blocking of the laser beam and demonstrate signal flanks with maximum amplitude (“cracking noise”, see figure 4 from 37s to 38s). This gives us information on the dynamic range of the system that is calculated to be about 14.5 dB above the intrinsic noise.

In the right half of figure 4 (b) the amplitude plot of the second part of the experiment is depicted. The transmission of the signal has been conducted through an already prepared solitary waveguide as a part of an array of solitons as before (see figure 3 (a)). To test the waveguiding features and the stability of the waveguide we start erasing the refractive index modulation by applying a strong white light illumination to the crystal (starting at 60s). This leads to vanishing of the waveguiding properties and therefore to a broad diffracted Gaussian beam at the crystal output face. Because of the spatial filtering with the small aperture at the crystal output face (shown in figure 3) the amplitude of the received signal at the detector is reduced to about 50 % during the erasure process (completed at 85s). Then less light is passing the filtering hole due to the broadened beam.

In agreement with earlier results [14] the coupling efficiency for the 632 nm beam in a solitary waveguide amounts to about 25 % without any special optimization like beam-to-numerical aperture matching. For the probe beam we have used a lens with 60 mm focus length to achieve a sufficiently small spot on the input face of the crystal while the working distance is large enough to integrate it into the existing system. The system allows for parallel transmission of multiple beams - in principle only limited by the number of waveguides written. Therefore, the single channel data rate can be multiplied with the number of independent channels. Additionally, possible wavelength multiplexing of signals in the same waveguide has not been investigated experimentally in this work.

The channel cross-coupling for modulated signals is already determined by the amount of light exchanged between neighbouring channels in the unmodulated case. Therefore, to minimize cross-coupling this has to be controlled. As already discussed in earlier works [14] interaction strength of solitons depends primarily on distance. Coherence and relative phase govern the actual type of interaction based on the overlapping electric fields of the involved beams. In the studied case of coherent in-phase beams propagating in parallel to form the arrays of solitons for this article beam-to-beam distance of 80  $\mu\text{m}$  has been set, which corresponds to about 3 to 4 beam diameters. This is a compromise between close packing and avoidance of strong attracting forces. Due to the large distance, the tails of the electric field in the overlapping region of neighbouring beams have dropped down enough to provide for separate solitary waveguides for every single beam. Along with the anisotropy of the refractive index modulation the waveguiding channels of gradient index type do only give rise to relevant cross-coupling

for much smaller distances of around 2 beam diameters where substantial interaction as well is present.

### C. Frequency analysis

The quality of information transport is also governed by the correct transmission of the Fourier components of the signal. To investigate the influence of the guiding on the signal quality we plotted each the amplitude and frequency analysis of the analyzed signals in figure 5. For comparison in the amplitude and frequency for a short part of the original signal used to modulate the guided laser beam is shown in the upper row (a).

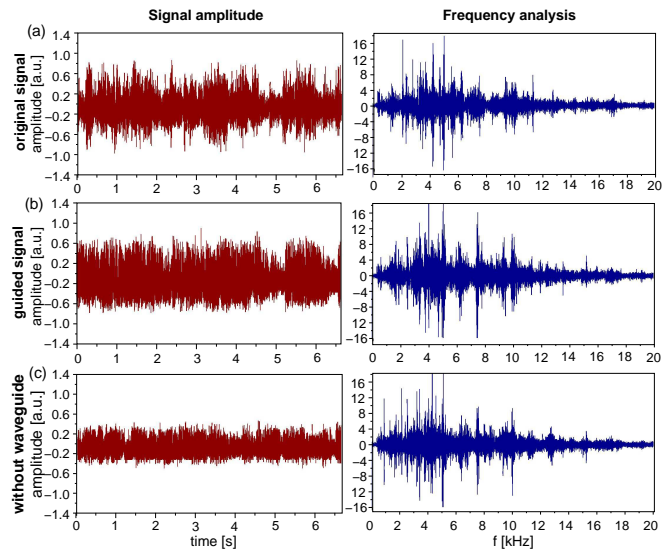


FIG. 5: Frequency analysis: The original signal used to modulate the guided laser beam is depicted in (a). In the middle row (b) the recorded signal guided in the solitary waveguide is shown, which represents the same part of the piece of music as in (a). Both shows basically also the same Fourier components. In the lower row (c) the case after waveguide removal is drawn. The frequency analysis on the right displays in principle the same frequency range for all three cases.

The recorded signal guided in the waveguide is depicted in the middle row (b). It represents the same portion of the piece of music as in (a) and the frequency plot does not show any significant difference. Compared with the the third row (c) where the recorded signal after waveguide removal is shown the amplitude of the guided signal (b) is about twice as large. Although the two parts represent two different positions in the transmitted piece of music the frequency range and the Fourier components are basically the same (right column in figure 5 (b) and (c)). Because the signal-to-noise ratio is different due to the lower signal amplitude with removed waveguide, the components of the noise are stronger present. The larger dynamic range of the original signal (a) is visible in the amplitude plot. It is limited for the transmitted signal in the experiment due to modulation and demodulation

losses and the higher noise level.

As a conclusion we can state that guiding in photorefractive soliton waveguides does not show significant influence on the characteristics of dynamically amplitude modulated signals. The principle suitability of single photorefractive solitons and complex arrays of these solitons for parallel optical data communication is therefore demonstrated.

#### IV. CONCLUSION

In this article we have shown successful transmission of dynamically modulated signals through solitary waveguides in photorefractive media. Analog modulation with an audio signal has been applied using a magneto-optical amplitude modulator setup and standard personal computer sound equipment has been used for analyzing the output. The short transmission distance of about 22 mm waveguide length demonstrates the principle adequacy of spatial photorefractive solitons to act as waveguides for dynamically amplitude modulated signals in different wavelength regions. The signal-to-noise ratio is sufficiently large to investigate the features of the system. We did not observe significant principle influences on the trans-

mission properties of modulated signals in our system.

Parallel transmission of modulated signals in neighbouring solitary waveguides has been demonstrated to be a novel tool for all-optical systems. Steered interaction and fusion [4] in combination with waveguiding in red and infrared wavelength region [8] are the other necessary building blocks needed for integration of all-optical switching devices in telecommunication applications using optical spatial solitons in photorefractive media. As a result all-optical data communication more and more gets a possible application of devices based on photorefractive solitons.

#### Acknowledgment

The authors like to thank Prof. Dr. Horst Dötsch from Fachbereich Physik, Universität Osnabrück, Germany, for the kind donation of magneto-optic crystal samples used to build the amplitude modulator. D.T. acknowledges support from Konrad-Adenauer-Stiftung e.V. Partial support from the Graduate School "Nichtlineare kontinuierliche Systeme" by DFG at Westfälische Wilhelms-Universität, Münster has been granted.

- 
- [1] C. Weinau, M. Ahles, J. Petter, D. Träger, and C. Denz. Spatial (2+1)-dimensional scalar- and vector-solitons in saturable nonlinear media. *Annalen der Physik*, 11:573–629, 2002.
- [2] Overview in 'Special issue on solitons', edited by M. Segev. *Opt. Photonics News*, 13:2, 2002.
- [3] Ming-feng Shih, Mordechai Segev, and Greg Salamo. Circular waveguides induced by two-dimensional bright steady-state photorefractive spatial screening solitons. *Opt. Lett.*, 21(13):931, 1996.
- [4] J. Petter, C. Denz, A. Stepken, and F. Kaiser. Anisotropic waveguides induced by photorefractive (2+1)d-solitons. *J. Opt. Soc. Am. B*, 19:1145–1149, 2002.
- [5] Ming-feng Shih, Zhigang Chen, Matthew Mitchell, Mordechai Segev, Howard Lee, Robert S. Feigelson, and Jeffrey P. Wilde. Waveguides induced by photorefractive screening solitons. *JOSA B*, 14(11):3091, 1997.
- [6] Andreas H. Carlsson, Johan N. Malmberg, Dan Anderson, Mietek Lisak, Eledna A. Ostrovskaya, Tristram J. Alexander, and Yuri S. Kivshar. Linear and nonlinear waveguides induced by optical vortex solitons. *Opt. Lett.*, 25(9):660, 2000.
- [7] M. Petrovic, D. Träger, A. Strinic, M. Belic, J. Schröder, and C. Denz. Solitonic lattices in photorefractive crystals. *Phys. Rev. E*, 68:055601R, 2003.
- [8] D. Träger, A. Strinic, J. Schröder, C. Denz, M. Petrovic, M. Belic, S. Matern, and H.-G. Purwins. Interaction in large arrays of solitons in photorefractive crystals. *J. Opt. A*, 5:518–523, 2003.
- [9] Marcus Asaro, Michael Sheldon, Zhigang Chen, Oksana Ostroverkhova, and W. E. Moerner. Soliton-induced waveguides in an organic photorefractive glass. *Opt. Lett.*, 30(5):519–521, 2005.
- [10] M. Peccianti, A. De Rossi, G. Assanto, A. De Luca, C. Umeton, and I. C. Khoo. Electrically assisted self-confinement and waveguiding in planar nematic liquid crystal cells. *Appl. Phys. Lett.*, 77(1):7, 2000.
- [11] D. N. Christodoulides, F. Lederer, and Y. Silberberg. Discretizing light behaviour in linear and nonlinear waveguide lattices. *Nature*, 424:817, 2003.
- [12] Denis Träger, Robert Fischer, Dragomir N. Neshev, Andrey A. Sukhorukov, Cornelia Denz, Wieslaw Krolikowski, and Yuri S. Kivshar. Nonlinear Bloch modes in two-dimensional photonic lattices. *arXiv*, nlin.ps:0601037, 2006.
- [13] J. Petter, J. Schröder, D. Träger, and C. Denz. Optical control of arrays of photorefractive screening solitons. *Opt. Lett.*, 28(6):438, 2003.
- [14] J. Petter and C. Denz. Guiding and dividing waves with photorefractive solitons. *Opt. Commun.*, 188:55, 2 2001.
- [15] Kind donation of Prof. Dr. Horst Dötsch at Universität Osnabrück, Germany.
- [16] Depending on this field the polarization is turned with typical values for the Faraday rotation constant of about  $1000^\circ \text{cm}^{-1}$  at  $1.3 \mu\text{m}$  and several  $10000^\circ \text{cm}^{-1}$  for visible wavelengths. The thin crystals created by liquid phase epitaxy have typical thicknesses of several  $10 \mu\text{m}$  which allows values for the resulting Faraday rotation near  $90^\circ$  only for relatively strong and homogeneous magnetic fields.
- [17] This configuration allows a modulation depth of the transmitted beam of around 30%.